Solid-State Electronics 120 (2016) 13–18

Contents lists available at ScienceDirect

Solid-State Electronics

journal homepage: www.elsevier.com/locate/sse

The influence of top electrode of InGaAsN/GaAs solar cell on their electrical parameters extracted from illuminated *I–V* characteristics

Wojciech Dawidowski [a,*], Beata Ściana [a], Iwona Zborowska-Lindert [a], Miroslav Mikolášek [b], Katarzyna Bielak [a], Mikołaj Badura [a], Damian Pucicki [a], Damian Radziewicz [a], Jaroslav Kováč [b], Marek Tłaczała [a]

[a] Faculty of Microsystem Electronics and Photonics, Wrocław University of Technology, 11/17 Janiszewskiego St., 50-372 Wrocław, Poland
[b] Institute of Electronics and Photonics, Faculty of Electrical Engineering and Information Technology, Slovak University of Technology, 3 Ilkovičova, 812 19 Bratislava, Slovakia

ARTICLE INFO

Article history:
Received 22 December 2015
Received in revised form 27 February 2016
Accepted 3 March 2016

The review of this paper was arranged by Prof. E. Calleja

Keywords:
Dilute nitrides
Solar cells
Illuminated *I–V* characteristics
Solar cell parameter extractions
Lambert W function

ABSTRACT

In the presented work the growth and fabrication process of dilute nitride based solar cells were reported. We fabricated three different solar cells to investigate the influence of top contact on their electrical parameters. Test devices were characterized by the means of current–voltage measurements carried out under the sunlight simulator. The obtained *I–V* results were scrutinized using a single diode equivalent circuit of a solar cell. We employed the Lambert W approach to find the solvable solution of the modified Shockley equation, in order to determine the basic solar cell electrical parameters such as: ideality factor n, series and shunt resistances (R_s and R_{sh}), saturation current I_0 and photocurrent I_{ph} generated in the solar cell structure. It was found that electrical parameters obtained from the fitting procedure depend on solar cell design. The type of top electrode influences the values of parasitic resistances, open circuit voltage and short circuit current.

1. Introduction

Photovoltaics (PV) is a promising source of a clean and carbon-free electricity. Beside well developed silicon PV which covers almost 90% of global market [1] the other technologies such as dye-sensitized [2] or thin film [3] solar cells are available. Especially thin film photovoltaics based on III–V semiconductors is interesting and perspective because of direct band gap and high value of absorption coefficient of these materials, which in turn reduces both the thickness of the absorber layer and the final cost of solar cell devices. Moreover, III–V solar cells are very attractive from the space and concentrator systems point of view [4].

Dilute nitride semiconductor alloys: GaAsN developed by Wayers in 1992 [5] and InGaAsN proposed by Kondow in 1996 [6] exhibit unusual properties. Partial substitution of arsenic with nitrogen atoms in GaAs host material has a tremendous effect on optical (drastic deterioration of luminescence, absorption red-shift), electrical (band gap reduction, split of the conduction band) and structural properties (lattice constant reduction) [7,8]. Uncommon features of dilute nitride alloys arise from a large electronegativity of N (3.04) compared with As (2.18) or Ga (1.81) and a big difference between atom radii of arsenic (115 pm) and nitrogen (65 pm). Introduction of indium into GaAsN alloy leads to the further band gap decrease and compensates stresses induced by nitrogen atoms. A precise control of indium and nitrogen contents in InGaAsN alloy enables tailoring the position of conduction band edge and band gap in wide range. Moreover, for some compositions (three times more indium than nitrogen) this quaternary alloy can be grown lattice-matched to gallium arsenide or germanium substrates and therefore it could become a material for the middle junction in multijunction solar cells [9]. Introducing InGaAsN-based subcell with a roughly 1–1.3 eV band gap to Ge–GaAs multijunction solar cell reduces the band discontinuity and improves light absorption in the range of 1.4–0.77 eV. Unfortunately, beside the widespread advantages of dilute nitride alloys there are several drawbacks associated with this material: high concentration of impurities (oxygen, carbon, hydrogen) and defects (vacancies, antisities, interstitials) which are the centers of the non-radiative recombination, miscibility gap between GaAs and GaN caused by significant difference in lattice constants [7].

* Corresponding author.
E-mail address: wojciech.dawidowski@pwr.edu.pl (W. Dawidowski).

http://dx.doi.org/10.1016/j.sse.2016.03.001
0038-1101/

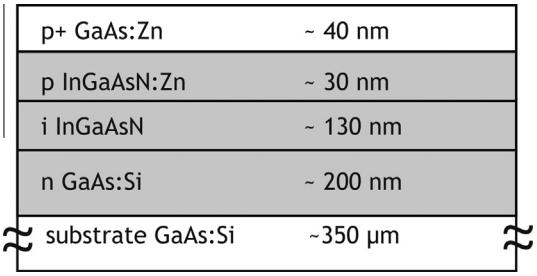

Fig. 1. Scheme of the epitaxial structure of InGaAsN/GaAs solar cell.

The main aim of this work is to investigate the influence of top solar cell electrode type on the electrical properties of the device. The investigated electrodes were prepared as ring metallic top contact and two partially transparent whole area contacts. Three solar cell devices, fabricated from the same epitaxial structure were characterized by the means of *I–V* measurement and the collected results were analyzed. We used Lambert W based, high accuracy method for determination of dilute nitride based solar cells parameters (n, R_s, R_{sh}, I_0 and I_{ph}). Obtained parameters were discussed and compared, moreover we connected the obtained results with solar cell design. It is worth mentioning we did not find in the literature any paper in which the parameters extraction of dilute nitride based solar cells using the Lambert W approach was discussed.

2. Growth and fabrication of heterojunction InGaAsN/GaAs solar cells

The structure of heterojunction p-i-n InGaAsN/GaAs solar cell was grown on silicon doped GaAs substrate by atmospheric pressure metalorganic vapour phase epitaxy (AP-MOVPE) using the AIX 200 R&D horizontal reactor. Trimethylgallium (TMGa–Ga $(CH_3)_3$), trimethylindium (TMIn–In$(CH_3)_3$), tertiarybutylhydrazine (TBHy–$(C_4H_9)HN_2H_2$) and 10% mixture of AsH_3 in hydrogen were used as sources of Ga, In, N and As, while diethylzinc (DEZn–Zn $(C_2H_5)_2$) and silane (20 ppm of SiH_4 in H_2) were employed as dopant sources. High purity hydrogen (99.9999%) was used as a carrier gas. The growth temperature varied from 585 to 670 °C

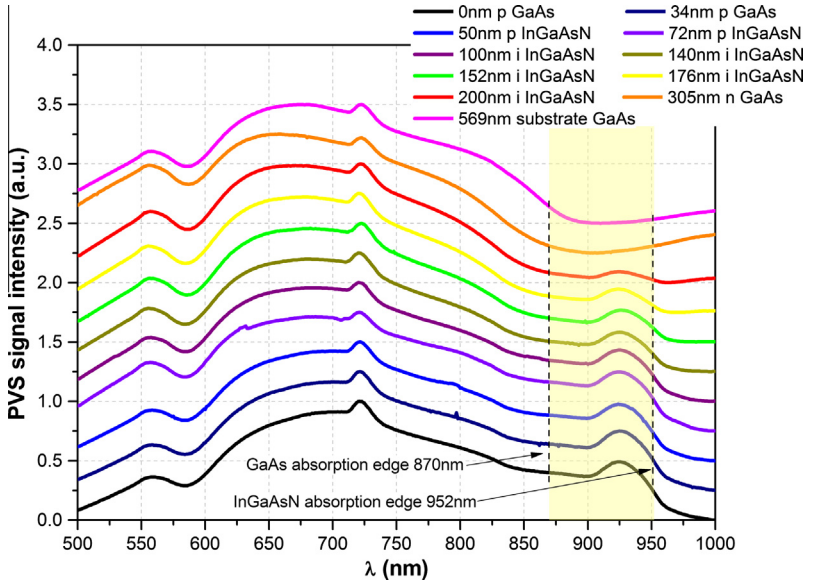

Fig. 2. Series of PVS spectra recorded during EC–V profiling of InGaAsN/GaAs heterostructure, at different etching depths.

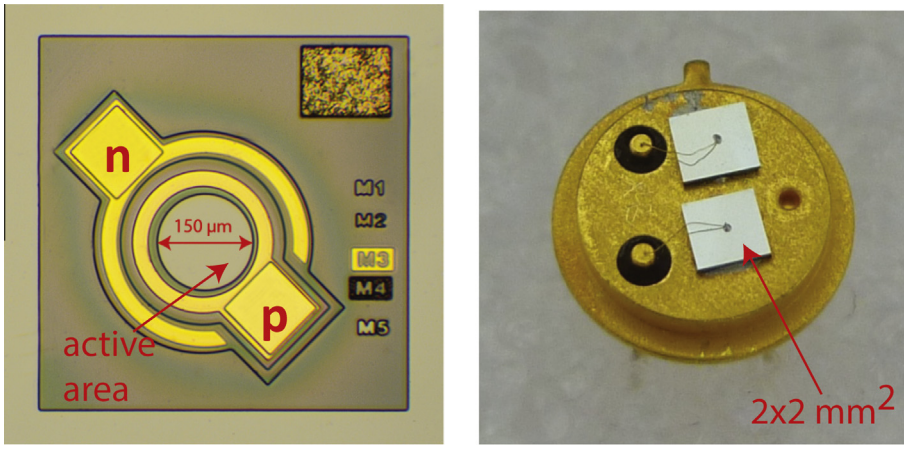

Fig. 3. Fabricated test solar cell devices: typical detector configuration (a) and with partially transparent p-type top electrode (b).

for InGaAsN and GaAs growth, respectively. More detailed information about the growth process optimization can be found elsewhere [10–13]. The epitaxial solar cell structure based on p-i-n junction (grey layers in Fig. 1) consists of undoped InGaAsN active region (with thickness about 130 nm) sandwiched between n-type GaAs buffer and p-type InGaAsN, capped by heavily doped p^+-GaAs contact layer. The InGaAsN bandgap was estimated to E_g = 1.283 eV based on the measured photoreflectance spectrum [12].

The absorption properties of epitaxial structure were examined by Photovoltage Spectroscopy (PVS) measurements. The applied PVS system is the part of Bio-Rad PN4300 electrochemical capacitance–voltage EC–V profiler. It records photovoltaic signal coming from illuminated Schottky junction created by analyzed semiconductor material and the suitable transparent electrolyte as a function of the wavelength of an incident illumination. Fig. 2 presents PVS spectra measured at a few selected etching depths of InGaAsN/GaAs heterostructure: from the surface of the epitaxial structure (0 nm depth), through p^+-GaAs:Zn (34 nm) and p-InGaAsN:Zn (50 nm), undoped i-InGaAsN (72, 100, 140, 152, 176 and 200 nm) to n-GaAs:Si buffer (305) or even the n^+-GaAs:Si substrate (569 nm). It is clearly visible that InGaAsN absorption edge (952 nm), obtained from the analysis of differential PVS signal, is shifted to longer wavelengths when compared to GaAs (about 870 nm). The highlighted region in Fig. 2 represents the absorption region of dilute nitride InGaAsN layer. Obtained PVS spectra reveals good optical quality of InGaAsN layer, what is confirmed by comparable shape of signals and its intensity.

In order to investigate the influence of the top electrode on solar cell properties three types of the test solar cell devices were fabricated. First one in a typical detector configuration with ring metallic top contact (as shown in Fig. 3a) labelled in this paper as solar cell A, and two others with partially transparent top electrode (B and C, depicted in Fig. 3b).

In the case of the solar cell A, the mesas were defined by combination of the optical lithography and wet chemical etching. Metallic n-type (AuGe/Ni/Au) and p-type (Pt/Ti/Pt/Au) contacts were deposited under vacuum conditions on the top and around the mesa. For solar cells depicted in Fig. 3b, p-type partially transparent AuBe metallization and AuGe/Ni n-type contact were deposited on the top and the bottom side of the structure, respectively. Transparency of the p-type top contact was determined on the basis of transmission measurements of the metal layer deposited on glass to be 5% (solar cell B) and 40% (solar cell C).

3. Analysis of the current–voltage characteristics

The fabricated solar cell devices were characterized by the means of current–voltage measurements (using Keithley 237 and Keithley 2612A instruments) under AM 1.5 spectrum with sunlight simulator Solar Light 16s-002. Basic solar cell parameters (open circuit voltage V_{OC}, short circuit current density j_{SC}, fill factor *FF* and conversion efficiencies η, η^*) of the fabricated test devices are collected in Table 1.

In the case of the solar cells B and C we calculated additional parameter η^*, which corresponds to the conversion efficiency with the assumption that AuBe top electrode is fully transparent.

Table 1
Basic parameters of the fabricated test solar cells.

Parameter	Solar cell A	Solar cell B	Solar cell C
V_{OC} (mV)	639.51	502.97	603.03
j_{SC} (mA/cm^2)	16.959	1.162	10.75
FF	0.704	0.568	0.711
η (%)	7.63	0.33	4.53
η^* (%)	–	6.64	11.32

3.1. Single diode model of solar cell

The simplest, one diode model describing ideal solar cell performance is the well-known Shockley equation. This relation becomes more complicated when the series (R_s) and shunt (R_{sh}) resistances are taking into account – the equation turns into the implicit function given as:

$$I = I_d + I_{sh} - I_{ph} = I_0 \exp\left(\frac{q(V - IR_s)}{nkT} - 1\right) + \frac{V - IR_s}{R_{sh}} - I_{ph}, \quad (1)$$

where I_d, I_{sh}, I_0 and I_{ph} are diode, shunt, saturation and photo currents, n is the ideality factor, k the Boltzmann's constant, T the absolute temperature, q the electronic charge. Fig. 4 shows the corresponding electrical model of a solar cell under illumination.

The implicit nature of modified Shockley equation raises difficulties and increases the complexity of standard parameter extraction, i.e. conventional curve fitting method. However, with the help of multivalued Lambert W function, which represents the solutions z of the equation $z = W(z)\exp W(z)$ for any real number z, the exact analytically solvable explicit equation for current I can be obtained [15–17]:

$$I = \frac{nkT}{qR_s} W_0\left[\frac{qR_s}{nkT}\left(I_{SC} - \frac{V_{OC}}{R_s + R_{sh}}\right)\exp\left(\frac{-qV_{OC}}{nkT}\right)\exp\frac{q}{nkT}\left(R_s I_{SC} + \frac{R_{sh}V}{R_s + R_{sh}}\right)\right] + \frac{V}{R_s} - I_{SC} - \frac{R_{sh}V}{R_s(R_s + R_{sh})}, \quad (2)$$

where W_0 stands for the basic branch of Lambert W function [14], V_{OC} the open circuit voltage and I_{SC} the short circuit current. For the calculation we will use only the values of principal branch of Lambert W function (denoted with blue line in Fig. 5) because only this branch satisfies the condition $W_0(0) = 0$.

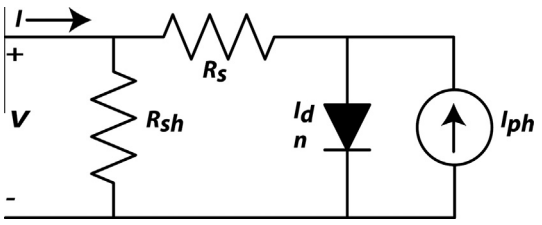

Fig. 4. One diode equivalent circuit of illuminated solar cell including diode and parasitic resistances.

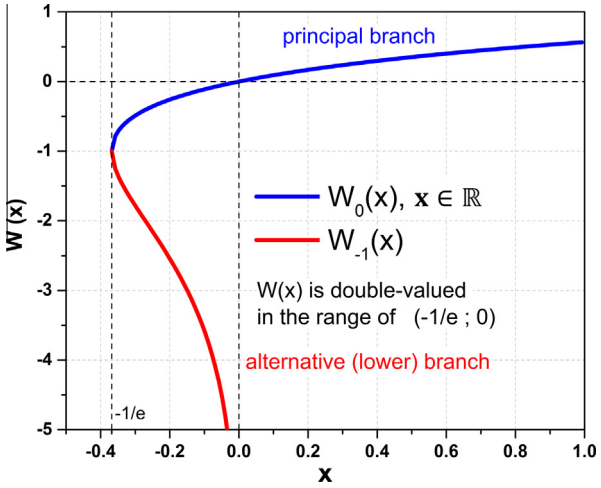

Fig. 5. Plots of two real branches of Lambert W function: principal $W_0(x)$ and alternative $W_{-1}(x)$.

We applied the Lambert W approach for extraction the basic parameters of heterojunction InGaAsN/GaAs solar cells based on illuminated *I–V* characteristics. Lambert W function is implemented in commercially available software, such as Matlab [18]. The n, R_s and R_{sh} parameters were extracted by using the least-squares method with Matlab's *lsqnonlin* function. The initial value of ideality factor parameter n was set to 1.5, while start values of R_s and R_{sh} parameters were estimated as a differential at open circuit voltage and short circuit current points, respectively [19]. Measured (open circle) and fitted *I–V* characteristics (red line) of InGaAsN/GaAs solar cell are shown in Fig. 6, additionally the residuals (defined here as the difference between measured and calculated current) for each solar cell are presented. After determination of n, R_s and R_{sh} parameters the saturation I_0 and photocurrent I_{ph} could be calculated according to equations [16]:

$$I_0 = \left(I_{SC} + \frac{R_s I_{SC} - V_{OC}}{R_{sh}}\right) \exp\left(\frac{-qV_{OC}}{nkT}\right) \tag{3}$$

$$I_{ph} = I_{SC} + \frac{R_s I_{SC}}{R_{sh}} - I_0. \tag{4}$$

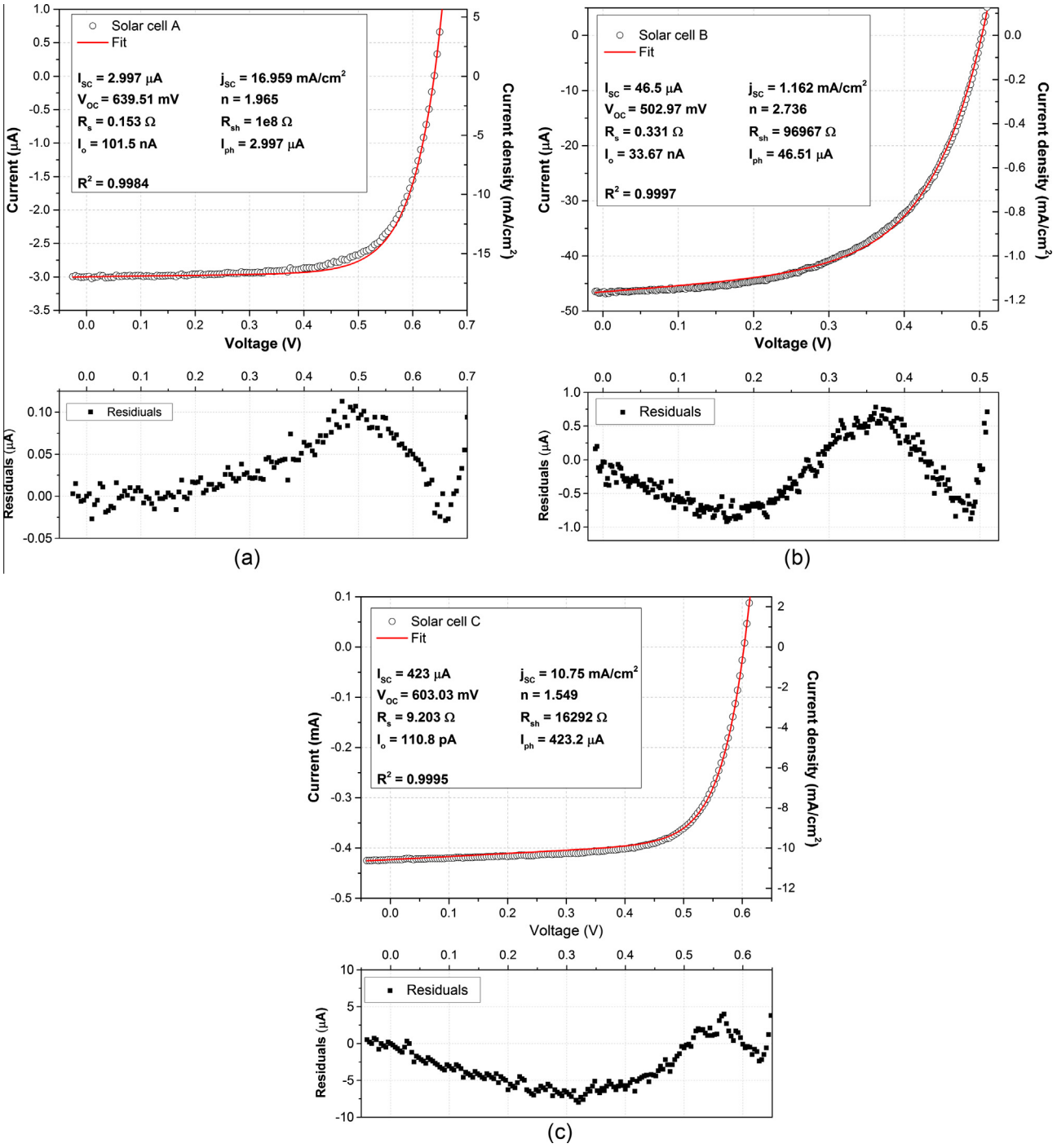

Fig. 6. Measured *I–V* characteristics of the investigated solar cells (open circle) with fitting curve (red line) and corresponding residuals plot for the solar cells A, B and C. (For interpretation of the references to colour in this figure legend, the reader is referred to the web version of this article.)

Table 2
Collected solar cell parameters determinated from *I–V* characteristics.

Parameter	Solar cell A	Solar cell B	Solar cell C
I_{SC} (μA)	2.997	46.5	423
j_{SC} (mA/cm^2)	16.959	1.162	10.75
V_{OC} (mV)	639.51	502.97	603.03
n	1.965	2.736	1.549
R_s (Ω)	0.153	0.331	9.203
R_{sh} (Ω)	1e8	96967	16292
I_0 (nA)	101.5	33.67	0.111
I_{ph} (μA)	2.997	46.51	423.2
R^2	0.9984	0.9997	0.9995

The values of all extracted parameters are collected in Table 2. The solar cell A with the top ring electrode (Fig. 6a) is characterized by the best electrical parameters – the largest: open circuit voltage (639.51 mV), short circuit current density (16.959 mA/cm^2), shunt resistance (100 MΩ) and the smallest: series resistance (0.153 Ω) and residuals (about 0.1 μA). In the case of the solar cell B (Fig. 6b) the series resistance R_s increases to 0.331 Ω and simultaneously shunt resistance R_{sh} decreases to almost 97 kΩ if compared with the solar cell A. Moreover, significant reduction of an open circuit voltage V_{OC} and a short circuit current density j_{SC} is observable, mainly due to a very low light transmission of the top electrode (5%). For the sample C (Fig. 6c) further increase of series and decrease of shunt resistances is clearly visible. V_{OC} and j_{SC} considerably increase to 603.03 mV and 10.75 mA/cm^2 because of 8-fold improvement of the top electrode transmittance, to 40%. The sample C is characterized by the lowest values of saturation current I_0 and ideality factor n.

Low value of n (1.549) factor indicates the presence of both phenomena responsible for a current flow in the junction: the diffusion of minority carriers and recombination current via point defect levels [20,21]. For the sample A the ideality factor almost reached 2, while for the solar cell B even exceed it (n = 2.736). High values of n may suggest that the current is dominated by recombination in the depletion region [21], which could be explained by non-radiative recombination through shallow or deep levels (trap-assisted recombination) [22]. All presented fits are in close agreement with the experimental data: the R-square parameter significantly exceed 99% and the residual is as low decimal parts of μA. Reduction of V_{OC}, J_{SC}, R_{sh} and increase of R_s and I_0 is connected with the properties of the top contact electrode of the investigated solar cells. For the solar cell A (with a ring shape top electrode) we achieved the best electrical parameters, while for devices with partially transparent top contacts the parameters become worse (increase of R_s, decrease of j_{SC} and V_{OC}). The obtained results explain why the fabrication of the top electrode should be optimized in order to obtain solar cells with good electrical parameters.

The applied method, proposed by Zhang is characterized by high accuracy. The fitting equation (Eq. (2)) was deprived of photo- and saturation current parameters, which usually differ more than five-six order of magnitude (the ratio I_{ph}/I_0 for solar cell C is more than 3.8×10^6) in order to avoid systematic error. According to detailed uncertainty analysis performed by Zhang the errors for extracted parameters are 0.1%, 50%, 5%, 3%, 50% for I_{ph}, I_0, n, R_s, R_{sh} obtained for input data burden with 5% noise signal. High error values for saturation current and shunt resistance are caused by poor influence of I_0 and R_{sh} on current described by Eq. (1), in comparison to I_{ph}, n and R_s [16].

4. Summary

In conclusion, the heterojunction InGaAsN/GaAs p-i-n solar cell structure was grown by AP-MOVPE on GaAs substrate. The three test devices (from the same epitaxial structure), with different top p-type metal contact were fabricated and characterized by the means of the current–voltage measurements. The detailed analysis of the obtained *I–V* curves employed single diode model of a solar cell combined together with Lambert W approach for solving the implicit equation was applied in order to determine the basic electrical solar cell parameters: n, R_s, R_{sh}, I_0 and I_{ph}. The fitting procedure of the measured *I–V* curves revealed the current flow mechanism through the junction which for our structures is mainly dominated by the recombination processes. Moreover, we found the correlation between the type of the top contact electrode and solar cell properties. For solar cell with ring top contact we obtain the highest j_{SC} and V_{OC} and the lowest value of series resistance, on the other hand this solar cell was characterized with the highest value of saturation current. Devices with semitransparent top electrode (solar cells B and C) are characterized by higher series and lower shut resistances (what deteriorates the open circuit voltage and short circuit current), while they exhibit lower value of saturation current.

Acknowledgements

This work was co-financed by Wrocław University of Technology statutory grants, by the European Union within European Regional Development Fund, through grant Innovative Economy POIG.01.01.02-00-008/08, by Slovak Grant Agency VEGA No. 1/0439/13 and Slovak-Polish International Cooperation Program no. SK-PL-0005-12.

References

[1] Saga T. Advances in crystalline silicon solar cell technology for industrial mass production. NPG Asia Mater 2010;2:96. http://dx.doi.org/10.1038/asiamat.2010.82.
[2] Grätzel M. Dye-sensitized solar cell. J Photochem Photobiol, C 2003;4:145–53. http://dx.doi.org/10.1016/S1389-5567(03)00026-1.
[3] Green MA. Thin-film solar cells: review of materials, technologies and commercial status. J Mater Sci: Mater Electron 2007;18:S15. http://dx.doi.org/10.1007/s10854-007-9177-9.
[4] Cotal H et al. III–V multijunction solar cells for concentrating photovoltaics. Energy Environ Sci 2009;2:174. http://dx.doi.org/10.1039/B809257E.
[5] Weyers M, Sato M, Ando H. Red shift of photoluminescence and absorption in dilute GaAsN layers. Jpn J Appl Phys 1992;31:L853. http://dx.doi.org/10.1143/JJAP.31.L853.
[6] Kondow M et al. GaInNAs: a novel material for long-wavelength-range laser diodes with excellent high-temperature performance. Jpn J Appl Phys 1996;35:1273. http://dx.doi.org/10.1143/JJAP.35.1273.
[7] Henini M. Dilute nitride semiconductors. 1st ed. Elsevier Science; 2004.
[8] Erol A. Dilute III–V nitride semiconductors and material systems: physics and technology. Springer; 2010.
[9] Sabnis V, Yuen H, Wiemer M. High-efficiency multijunction solar cells employing dilute nitrides. In: AIP Conf. Proc. vol. 1477, no. 14; 2012. http://dx.doi.org/10.1063/1.4753823.
[10] Ściana B, et al. Influence of the AP MOVPE process parameters on properties. In: Proc. of SPIE. vol. 8902; 2013, 89020J-1. http://dx.doi.org/10.1117/12.2031055.
[11] Ściana B et al. MOVPE growth of AIIIBV-N semiconductor compounds for photovoltaic applications. Cryst Res Technol 2012;47(3):313–20. http://dx.doi.org/10.1002/crat.201100415.
[12] Dawidowski W et al. AP-MOVPE technology and characterization of InGaAsN p-i-n subcell for InGaAsN/GaAs tandem solar cell. Int J Electron Telecommun 2014;60(2):151–6. http://dx.doi.org/10.2478/eletel-2014-0018.
[13] Dawidowski W, et al. Influence of rapid thermal annealing on optical properties of (In,Ga)(As,N)/GaAs quantum wells. In: Proc. of SPIE. vol. 8902; 2013, 89022G-1. http://dx.doi.org/10.1117/12.2031065.
[14] Corless RM et al. On the Lambert W function. Adv Comput Math 1996;5:329. http://dx.doi.org/10.1007/BF02124750.
[15] Ortiz-Conde A et al. New method to extract the model parameters of solar cells from the explicit analytic solutions of their illuminated IV characteristics. Sol Energy Mater Sol Cells 2006;90:352.
[16] Zhang C et al. A simple and efficient solar cell parameter extraction method from a single current–voltage curve. J Appl Phys 2011;110:064504. http://dx.doi.org/10.1016/j.solmat.2005.04.023.
[17] Jung W, Guziewicz M. Schottky diode parameters extraction using Lambert W function. Mater Sci Eng, B 2009;165:57. http://dx.doi.org/10.1016/j.mseb.2009.02.013.

[18] MATLAB and Statistics Toolbox Release. Natick, Massachusetts, United States: The MathWorks, Inc.; 2009.
[19] Ghani F et al. The numerical calculation of single-diode solar-cell modelling parameters. Renewable Energy 2014;72:105–12. http://dx.doi.org/10.1016/j.renene.2014.06.035.
[20] Breitenstein O, et al. The origin of ideality factors $n > 2$ of shunts and surfaces in the dark *I–V* curves of Si solar cells. In: Proc. 21st European photovoltaic solar energy conference, Dresden; 2006. p. 625–8.
[21] Mialhe P et al. The diode quality factor of solar cells under illumination. J Phys D: Appl Phys 1986;19:483–92. http://dx.doi.org/10.1088/0022-3727/19/3/018.
[22] Breitenstein O, et al. Interpretation of the commonly observed I–V characteristics of C-SI cells having ideality factor larger than two. In: Proc. 4th IEEE World Conf. Photovoltaic Energy Conversion; 2006. p. 879–84, http://dx.doi.org/10.1109/WCPEC.2006.279597.